An Experimental Thermal Time-Constant Correlation for Hydraulic Accumulators

A. Pourmovahed[1]

D. R. Otis

Mechanical Engineering Department,
University of Wisconsin-Madison,
Madison, WI 53706

A thermal time-constant correlation based on experimental data is presented for gas-charged hydraulic accumulators. This correlation, along with the thermal time-constant model, permits accurate prediction of accumulator thermodynamic losses and the gas pressure and temperature history during compression or expansion. The gas is treated as a real gas, and all properties are allowed to vary with both pressure and temperature. The correlation was developed from heat transfer data obtained with a 2.5 liter piston-type accumulator charged with nitrogen gas. Both horizontal and vertical orientations were studied. The experiments covered the range, $2.6\times10^{8}<Ra^{*}<9.5\times10^{10}$, $0.77<L/D<1.50$, *and* $0.71<T^{*}<1.0$. *The gas pressure was varied between 1.0 and 19.5 MPa.*

Introduction

A hydraulic accumulator in a pressure vessel that can hold a relatively large volume of hydraulic fluid under pressure. It is used in a wide variety of applications as an energy storage device, a pulsation damper, a surge suppressor, a thermal-expansion compensator, or an emergency power source.

The gas-charged accumulator is usually a cylindrical or spherical vessel with a piston, bladder, or diaphragm separating the oil from the charge gas. It utilizes the compressibility of the gas (usually nitrogen) to store energy. The gas-charged hydraulic accumulator has proved to be much more practical than the weight- or spring-loaded type and is preferred for most hydraulic systems due primarily to its lighter weight, lower cost, and compactness. A piston-type gas-charged hydraulic accumulator is schematically shown in Fig. 1. It consists of a precision machined cylinder and a freely moving piston which serves as a barrier between the oil and the charge gas.

Selection of accumulator size and precharge pressure has been the subject of studies done by many researchers. If the accumulator is too small, it cannot return sufficient oil to the system and the performance specifications of the system may not be met. On the other hand, an oversized accumulator can be costly or too heavy for some applications such as hybrid-vehicle powertrains or aircraft landing-gear systems.

Available energy is lost in hydraulic accumulators due to irreversible heat transfer. A typical charge-gas pressure-volume history resulting from a sinusoidal variation of oil flow is shown in Fig. 2. Upon oil inflow, the charge gas is compressed and its temperature rises. During this process, heat is convected to the walls and conducted away through the cylinder materials. The transfer of heat is across a finite temperature difference, and entropy is produced. During gas expansion, heat is transferred in the opposite direction. The average gas pressure during expansion is less than that during compression, and the area enclosed by the hysteresis loop (the p-V diagram) is equal to the net availability loss for the cycle. The net heat loss from the cycle is equal to this destruction of available energy.

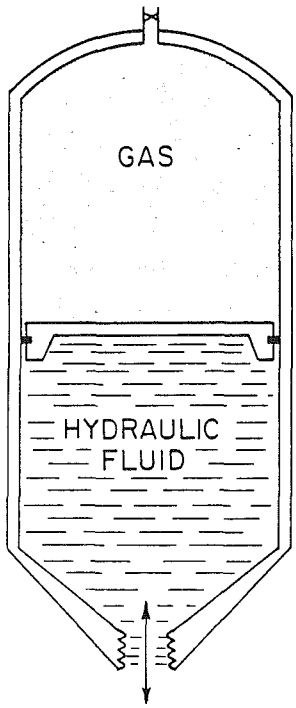

Fig. 1 A piston-type hydraulic accumulator

[1]Currently, Assistant Professor, Mechanical Engineering Department, Lawrence Technological University, Southfield, Mich.

Contributed by the Dynamic Systems and Control Division for publication in the JOURNAL OF DYNAMIC SYSTEMS, MEASUREMENT AND CONTROL. Manuscript received by the Dynamic Systems and Control Division December 1985; revised manuscript received July 1986. Associate Editor: D. Limbert.

Copyright © 1990 by ASME
Downloaded 28 Oct 2008 to 142.58.187.30. Redistribution subject to ASME license or copyright; see http://www.asme.org/terms/Terms_Use.cfm

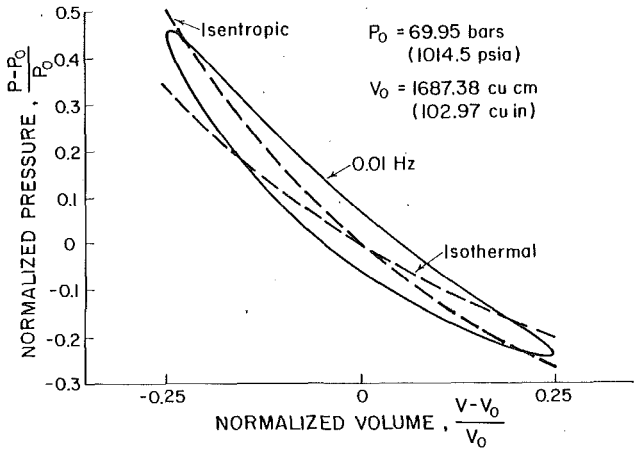

Fig. 2 Typical pressure-volume history for sinusoidal piston motion at 0.01 Hz. Isothermal and isentropic processes are also shown.

Predicting the performance of hydraulic accumulators requires some knowledge of the thermodynamic processes experienced by the charge gas. Since the gas is, for most practical cases, at a relatively high pressure, it should be treated as a "real gas." Historically, however, a combination of ideal gas assumptions and safety factor oversizing methods have been used in selecting hydraulic accumulators. A common practice is to assume that the processes involved are isothermal, adiabatic, or polytropic. This simply means that the thermal losses are ignored and the accumulator is modeled as a "spring." Furthermore, the vaule of the polytropic exponent used in the calulations is often unknown, and designers have used different "rules of thumb" which have proven in some cases to be inaccurate. A study by Beachley (1973) shows that for rapid expansion of nitrogen gas, the value of the polytropic exponent may exceed 2.0 if nonideal gas properties are considered.

Otis (1973) has developed a heat convection model to describe the thermodynamic processes of the charge gas. Instead of using the conventional methods (which employ the polytropic relations, $pV^n = \text{constant}$), an energy balance was made on the gas and the rate of heat transfer was assumed proportional to the surface area and the difference between the wall temperature and the average gas temperature. This resulted in a "thermal time-constant model" which will be discussed in the next section.

A conduction model has been presented by Svoboda et al. (1978). This model can be used to calculate the thermal time constant. This thermal model assumes that the heat convection process is "similar" to heat conduction in a solid if a proper "effective" thermal diffusivity is used.

The Thermal Time-Constant Model

Considering the charge gas as a closed system, an energy balance can be made as follows:

$$m_g \frac{du}{dt} = hA_w(T_w - T) - p\frac{dV}{dt} \tag{1}$$

where A_w is the effective area of the accumulator for heat convection. For a real gas, the internal energy per unit mass, u, is given by,

$$du = c_v dT + \left[T\left(\frac{\partial p}{\partial T}\right)_v - p\right]dv \tag{2}$$

Combining equations (1) and (2), we obtain,

$$\tau\frac{dT}{dt} + T = T_w - \frac{T\tau}{c_v}\left(\frac{\partial p}{\partial T}\right)_v \frac{dv}{dt} \tag{3}$$

with

$$\tau \equiv \frac{m_g c_v}{hA_w} \tag{4}$$

The thermal time constant, τ, must be measured for the particular accumulator and range of operation; or it may be estimated using heat transfer models. The purpose of this paper is to present experimental correlations for cylindrical accumulators oriented in the horizontal or vertical position. It must be mentioned that τ is not really a constant since the convection heat transfer coefficient, h, and the effective wall area, A_w, both change with time. However, as shown by Pourmovahed and Otis (1984, 1985) a constant does in fact fit experimental data quite well.

The gas pressure is related to the gas temperature and specific volume by the Benedict-Webb-Rubin (BWR) equation of state (Cooper et al., 1967 and Kerr, 1986).

$$p = \frac{RT}{v} + (B_0RT - A_0 - C_0/T^2)/v^2 + (bRT - a)/v^3 + a\alpha/v^6 + (c(1+\gamma/v^2)e^{-\gamma/v^2})/v^3T^2 \tag{5}$$

The above equation was shown to be in remarkable agreement with the data published by the NBS for nitrogen (Jacobsen et al., 1973) for the entire range of interest for accumulator applications (Pourmovahed, 1985). Combining equations (3) and (5) yields,

Nomenclature

A_0, a, B_0, b, C_0, c = BWR constants
A_w = total internal surface area exposed to gas
c_v = gas specific heat at constant volume
D = cylinder internal diameter
F = function of L/D, equation (11)
g = acceleration of gravity
h = overall heat transfer coefficient
k = gas thermal conductivity
L = length of cylinder exposed to gas
m_g = mass of the gas
Nu = Nusselt number
n = polytropic exponent
p = gas pressure
R = ideal gas constant
Ra* = instantaneous modified Rayleigh number, equation (8)
T = gas mixed-mean temperature
T^* = temperature ratio, equation (9)
T_{max} = maximum gas temperature
T_w = spatially averaged wall temperature
t = time
u = internal energy per unit mass
V = gas volume
v = gas specific volume ($=1/\rho$)
Z = characteristic length, equation (10)
α = BWR constant
β = coefficient of thermal expansion
γ = BWR constant
μ = gas viscosity
ρ = spatially averaged gas density
σ = see equation (21)
τ = thermal time constant
τ^* = dimensionless thermal time constant, equation (12)

Downloaded 28 Oct 2008 to 142.58.187.30. Redistribution subject to ASME license or copyright; see http://www.asme.org/terms/Terms_Use.cfm

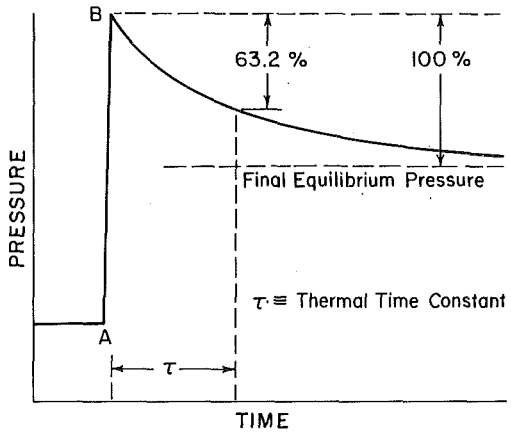

Fig. 3 Pressure relaxation at constant volume after a rapid compression

$$\frac{dT}{dt}=\frac{T_w-T}{\tau}-\frac{1}{c_v}\left\{\frac{RT}{v}\,(1+b/v^2)+\frac{1}{v^2}\,(B_0RT+2C_0/T^2)\right.$$

$$\left.-\frac{2c}{v^3T^2}\,(1+\gamma/v^2)e^{-\gamma/v^2}\right\}\frac{dv}{dt} \qquad (6)$$

Equation (6) is the energy equation for the gas and can be integrated to predict gas temperature and pressure history for a process or cycle. The algorithm presented by Otis and Pourmovahed (1985) is based on this approach.

Measuring the Thermal Time Constant

The thermal time constant can be measured experimentally by observing the gas pressure response to a step change in the gas volume. Figure 3 is a plot of the charge-gas pressure versus time for the process described above. During the constant-volume pressure relaxation, the gas temperature is given by (see equation (6)),

$$\ln\frac{T-T_w}{T_{\max}-T_w}=-\frac{t}{\tau} \qquad (7)$$

The thermal time constant, τ, is the time it takes for the gas pressure (or temperature) to drop by 63.2 percent. This is shown graphically in Fig. 3.

The purpose of this work is to present an experimental thermal time-constant correlation for hydraulic accumulators in horizontal or vertical orientation. This correlation can be used to estimate the time-constant for gas-charged accumulators. It eliminates the need for experimental evaluation of this constant.

The Apparatus

The test accumulator is a piston-type, gas-charged, hydraulic accumulator with a maximum gas volume of 2.5 liters (see Fig. 4). The 12.38-cm-diameter piston (maximum stroke = 13.79 cm) is driven by a 20.7-MPa (3000 psi), 0.17-liter/s (2.7 gpm) hydraulic power supply, and an electronic controller sets the position of a hydraulic servovalve to provide the desired motion. The hydraulic drive system is capable of operation to 50 Hz. The apparatus is described in detail by Pourmovahed (1985).

The gas pressure is measured with a Wiancko 0 to 27.6-MPa (0–4000 psia) variable reluctance transducer (Model P2-3090-1) with a 0 to 5-v linear output which has a maximum error of ±0.003 MPa due to noise and hysteresis. It was calibrated for each experiment using a 30.48-cm (12 in) Heise gage (0–20.7 MPa) with a least count of 0.02 MPa.

The gas volume signal comes from a 10-turn potentiometer which is connected to the piston by a rack and pinion, and the position was calibrated by a steel ruler permanently affixed to the apparatus with a least count of 0.0254 cm (0.01 in) yielding a probable error of 0.003 liters.

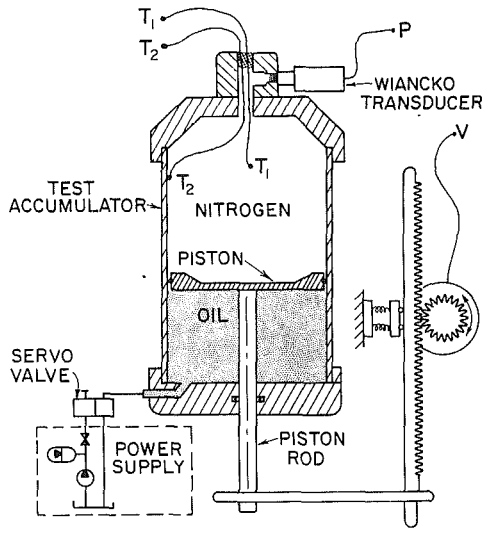

Fig. 4 Schematic of the test setup showing the location of thermocouples, pressure transducer and volume transducer. The volume transducer provides the feedback for the servovalve controller (not shown).

The gas temperature thermocouple was constructed of 0.013-cm-diameter copper-constantan wires welded to form a spherical junction of 0.036-cm-diameter. It was located 7.0 cm below the endcap.[2] The wall temperature was measured with a copper-constantan thermocouple constructed of 0.051-cm-diameter wire, twisted together and soft-soldered to the inside wall, 8.0 cm below the endcap.

The gas temperature, volume, pressure, and the wall temperature were recorded on a 4-channel Nicolet 4094 digital storage oscilloscope (time/point = 20 ms) and the data were stored permanently on floppy disks. The thermocouple outputs were amplified 50 times before connection to the scope.

The Procedure

The enclosure was first precharged with nitrogen gas to the desired pressure and the gas was then allowed to temperature stabilize with the room after which the precharge pressure was measured. Using a signal generator, a triangular wave was first connected to an amplifier. The output of this amplifier was then used to drive the control system. By saturating this amplifier, it was possible to rapidly compress the gas with the desired piston velocity and then keep the gas volume constant for a long time. The piston velocity and stroke were varied by turning the frequency or amplitude knobs on the signal generator, respectively.

With the cylinder in the vertical position, 35 test runs were made covering the following range:

Precharge pressure:	1–9 MPa, gage
L/D after compression:	0.77–1.50
Average piston velocity:	0.11–8.08 cm/s

For the horizontal orientation, 18 test runs covered the range:

Precharge pressure:	2.1–7.8 MPa, gage
L/D after compression:	0.77–1.50
Average piston velocity:	0.30–7.44 cm/s

The experimental data for run number 22 is shown in Fig. 5. A complete set of the observed data and results have been documented by Pourmovahed (1985).

Processing the Observed Data

To compute the thermal time constant and the temperature

[2]This position was chosen to locate the gas thermocouple in the middle of the gas enclosure for $L/D = 1.0$.

Downloaded 28 Oct 2008 to 142.58.187.30. Redistribution subject to ASME license or copyright; see http://www.asme.org/terms/Terms_Use.cfm

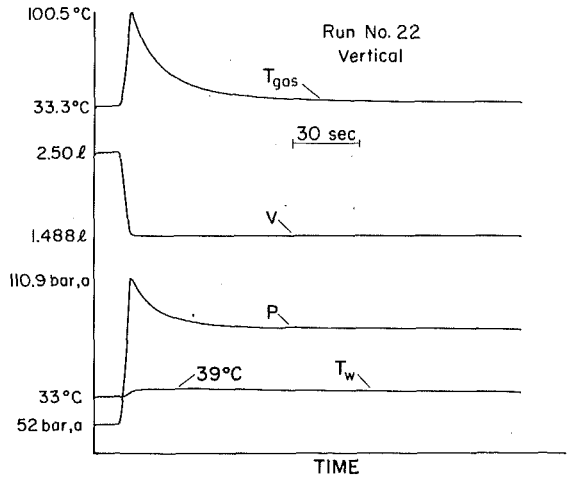

Fig. 5 Gas temperature, volume, pressure, and wall temperature history for run number 22

history for the gas, it is necessary to analyze the decay of pressure with time after the gas is compressed to its final volume (see Fig. 5). The procedure is outlined below:

1. At discrete times, the instantaneous gas pressure was read from the signal stored on floppy disks. The time interval used was either 5 or 10 seconds (oscilloscope sampling time interval was 20 ms). The pressure at any time interval was then computed from the proper pressure calibration line.
2. The mass of nitrogen was found from the gas pressure, temperature, and volume before compression. The equation of state used was that of the NBS (Jacobsen et al., 1973).
3. Knowing the final gas volume and mass of nitrogen, the specific volume (or density) of the gas is calculated. This mixed-mean density remains constant throughout the cooling process.
4. At any given time, t, the mixed-mean temperature of the gas, T, was computed from the specific volume and pressure using the equation of state for nitrogen (Cooper et al., 1967).
5. The thermal time constant, τ, was then found from the temperature versus time data as described earlier in this paper (see Fig. 3).[3]

Dimensionless Parameters

To correlate the time-constant data, it is necessary to determine the pertinent dimensionless parameters. Since natural convection is responsible for heat transfer within the gas enclosure, Rayleigh number is obviously an important parameter. The other significant parameters are the length/diameter ratio (L/D) and the wall/gas temerature ratio (T_w/T). The dimensionless parameters were defined as follows:

$$\mathrm{Ra}^* \equiv \frac{\rho^2 g\beta(T-T_w)Z^3 c_v}{\mu k} \tag{8}$$

$$\mathrm{T}^* \equiv \frac{T_w}{T} \tag{9}$$

In equation (8), Z is the characteristic length given by,

$$Z \equiv L \text{ for vertical orientation}$$
$$Z \equiv D \text{ for horizontal orientation} \tag{10}$$

The L/D parameter should be included in the analysis to account for the end effects (heat transfer to the endcap and the piston). It is obvious that as the L/D ratio increases, the end effects become less significant. It seems reasonable to construct the following geometric ratio:

$$F \equiv (V/A_w D) = \frac{(L/D)}{2+4(L/D)} \tag{11}$$

The parameter F is equal to the gas volume/(surface area x diameter). The temperature ratio, T^*, accounts for the temperature variation within the gas which in turn results in a spatial variation in the gas properties.

During the cooling process, the gas mass and volume are constant. This means that in equations (8) through (11), L, D, ρ, g, and Z are constant. The gas pressure, p, and the spatially averaged gas temperature, T, decrease with time (see Fig. 3). The decrease in the gas pressure and temperature will result in a change in the gas properties. Therefore, T, T_w, β, μ, and k will vary during the process.

The dimensionless thermal time-constant is defined as,

$$\tau^* \equiv \frac{k\tau}{\rho c_v Z^2} \tag{12}$$

It is expected that τ^* will be a function only of the parameters defined earlier, namely,

$$\tau^* = f(\mathrm{Ra}^*, L/D, F, T^*) \tag{13}$$

and it is further assumed that,

$$\tau^* = C\ \mathrm{Ra}^{*n_1}(L/D)^{n_2} F^{n_3} T^{*n_4} \tag{14}$$

or

$$\ln(\tau^*) = \ln(C) + n_1\ln(\mathrm{Ra}^*) + n_2\ln(L/D) + n_3\ln(F) + n_4\ln(T^*) \tag{15}$$

where C, n_1, n_2, n_3, and n_4 are constants and must be determined from the experimental data.

The Results

The 35 vertical test runs resulted in 35 values for each of the variables in equation (15). For simplicity in use of the correlations, all dimensionless parameters in equation (15) were *evaluated at the beginning of the cooling process* (right after the rapid compression).[4] To fit the data, a multiple regression method was implemented by using the Minitab program. This resulted in the following correlation if all gas properties are evaluated at the gas mixed-mean temperature:

$$\tau^* = 0.045\ \mathrm{Ra}^{*-0.260}\left(\frac{D}{L}\right) F^{-1.156}\ T^{*1.170} \tag{16}$$

The thermal time constant, τ, actually varied from 7.5 to 30.0 s.[5]. Figure 6 shows the experimental τ^* versus that calculated from equation (16) for all vertical test runs. It should be noted that each test run results in a single value of τ^*.

The data obtained for the 18 horizontal runs were processed in a manner similar to the vertical case. The characteristic length, Z, was set equal to the cylinder diameter, D, and the following correlation was obtained:

$$\tau^* = 4.474\ \mathrm{Ra}^{*-0.305}\ F\ T^{*0.223} \tag{17}$$

Experimental values of τ^* are plotted versus those computed from equation (17) in Fig. 7. The thermal time constant for the horizontal cylinder varied from 11.5 to 25.9 s. For comparison, the data of Svododa et al. (1978) for rapid expansion

[3]The time constant can be measured from either the pressure or the temperature history for the gas. Mathematically, it is more appropriate to use the temperature data. Note that at low pressures the ideal gas law is applicable and the value of τ will be the same no matter which method is chosen.

[4]Note that during the cooling process in a single test run, L/D, F, and τ^* stay constant while Ra^* and T^* vary with time.

[5]The time constant for run number 20 was 55.2 s. For this test run, the piston velocity was unusually low. This will be discussed in the following section.

Downloaded 28 Oct 2008 to 142.58.187.30. Redistribution subject to ASME license or copyright; see http://www.asme.org/terms/Terms_Use.cfm

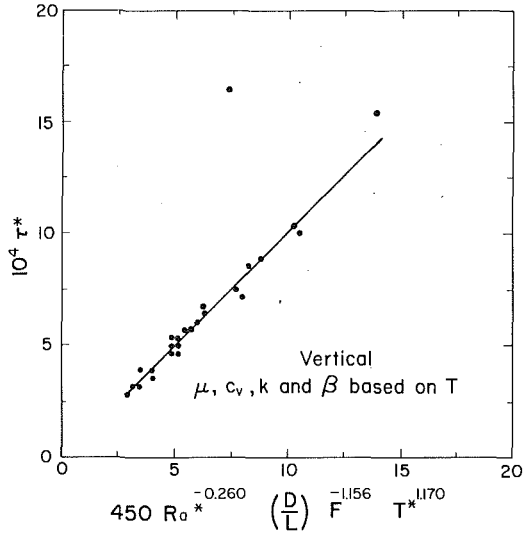

Fig. 6 Dimensionless thermal time constant versus that computed from equation (16) for the vertical cylinder. Ra* and T^* are evaluated at the beginning of the cooling process.

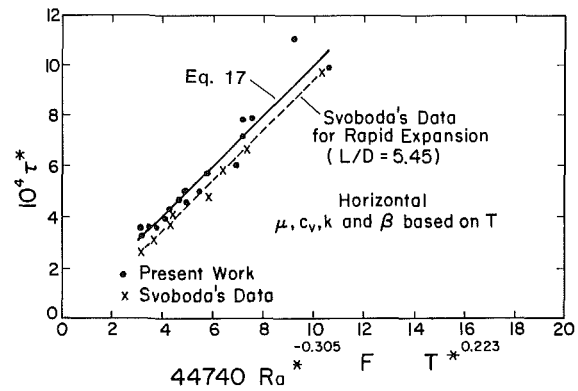

Fig. 7 Dimensionless thermal time constant versus that computed from equation (17) for the horizontal cylinder. Ra and T^* are evaluated at the beginning of the cooling process. Data of Svoboda et al. (1978) for rapid expansion are also shown.

of the gas is also shown in Fig. 7. Their data is for a 28.4 liter accumulator with $L/D = 5.45$. They varied the precharge pressure from 3.45 to 10.35 MPa (500 to 1500 psig).

Effect of Piston Velocity on τ

It was proposed in previous sections that in correlating the thermal time-constant data, the piston velocity during compression (or the Reynolds number) may be left out. To examine this assumption, 14 test runs were made with the cylinder in the vertical position (runs 11 through 24). The cylinder was precharged with nitrogen to 5.03 MPa, gage and the gas was compressed from 2.50 to 1.448 liters ($L/D = 1.0$ after compression). The time for compression was varied from 1.04 to 80 s. The thermal time constant for runs 11 through 24 is plotted versus piston velocity in Fig. 8. It is seen from this figure that as the piston velocity increases, the thermal time constant decreases rapidly and reaches a plateau. Since the time constant is insensitive to the piston velocity when the compression is rapid, it can be concluded that forced convection does not play a major role in this process. As the piston velocity becomes small, τ increases dramatically. This can be attributed to the aging of the boundary layer. For the data point with $\tau = 55.2$ s, the time for compression was 80 s. By the time the piston stopped moving in this test run, most of the heat had already been transferred from the gas and the boundary layer had aged. Therefore, one should expect a low heat

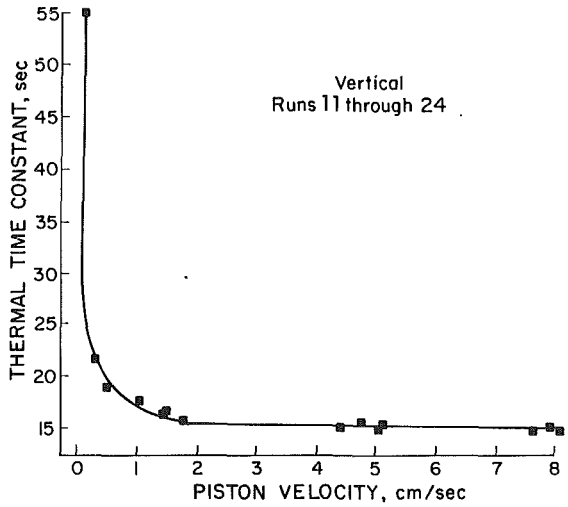

Fig. 8 Experimentally measured thermal time constant versus average piston velocity for runs 11 through 24. The Reynolds number varies form 625 to 43655.

transfer coefficient and a large time constant. The data point mentioned above does not correlate with the remainder of the data as can be seen from Fig. 6. The conclusion made from the above is that the piston velocity is not important in correlating the time-constant data so long as it is not too small (Reynolds number less than 5000).

Temperature Decay Curves

Using the thermal time-constant model, it is possible to predict the relaxation (cooling) process for the gas after a rapid compression (or expansion). The rate of change of the gas temperature, T, during the constant-volume cooling process is given by (see equation (6)),

$$\frac{dT}{dt} = \frac{T_w - T}{\tau} \tag{18}$$

The convection heat transfer coefficient for a *vertical* accumulator is given by [6],

$$\mathrm{Nu} \equiv \frac{hL}{k} = 1.6151\ \mathrm{Ra}^{*0.344} F^{1.760} T^{*\,-2.528} \tag{19}$$

The above equation was developed by Pourmovahed (1985) based on the heat transfer data obtained during the experiments that led to the thermal time-constant correlations given in equations (16) and (17). The parameters Ra* and T^* are the instantaneous Rayleigh number and temperature ratio as defined in equations (8) and (9). It must be noted that these parameters vary during the cooling process of the gas indicating that the heat transfer coefficient, h, is not a constant. One would therefore conclude that the thermal time constant, τ, should also vary during a process! It must be emphasized that in reality τ does change with time and should be allowed to vary if extreme accuracy is necessary in the analysis. However, in many cases, good accuracy is achieved with a single value of τ for the overall process.

Combining equations (19), (8), and (4) yields,

$$\tau = \frac{m_g L \sigma}{1.6151\ A_w} F^{-1.760} T^{*2.528} \left[\rho^2 g L^3 (T - T_w)\right]^{-0.344} \tag{20}$$

with

$$\sigma \equiv \left(\frac{c_v}{k}\right)^{0.656} (\beta/\mu)^{-0.344} \tag{21}$$

It should be noted that during the cooling process m_g, L, A_w,

[6] The corresponding equation for a horizontal accumulator is given by Pourmovahed (1985).

Downloaded 28 Oct 2008 to 142.58.187.30. Redistribution subject to ASME license or copyright; see http://www.asme.org/terms/Terms_Use.cfm

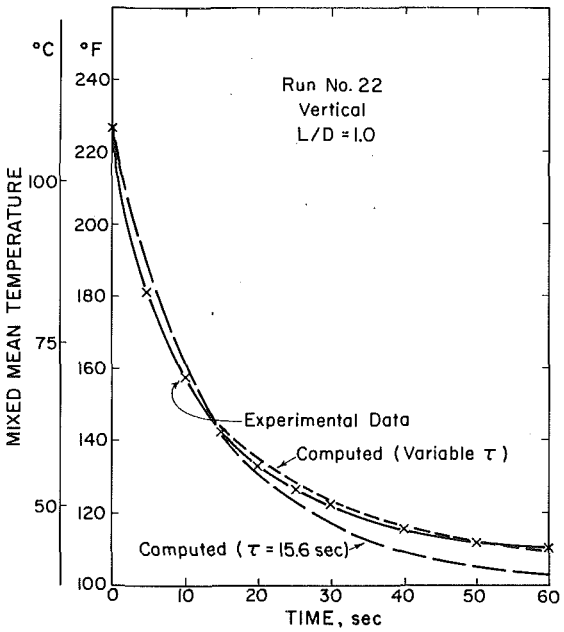

Fig. 9 Mixed-mean temeprature history for run number 22

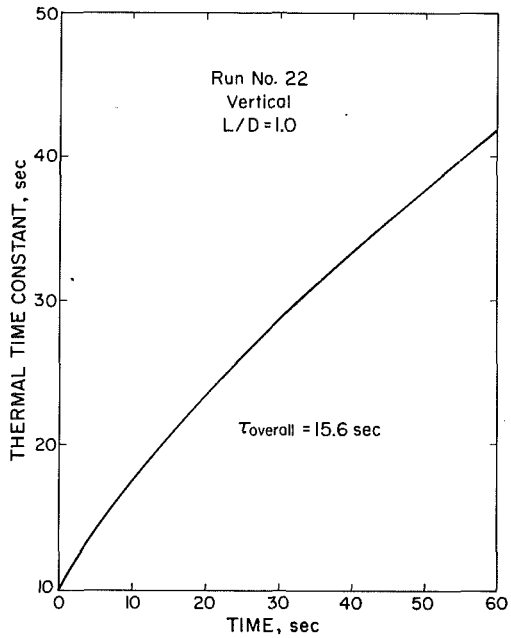

Fig. 10 Thermal time constant versus time for run number 22

F, ρ, and g stay constant while σ, T^*, T, and T_w vary with time.[7]

Equations (18), (20), and (21) were used to predict the gas temperature history for run number 22. The value of σ was found to be,

$$\sigma = 132.8 \left(\frac{m-s}{kg}\right)^{0.312} {}^\circ\mathrm{K}^{0.344} \quad @t=0$$

$$\sigma = 126.3 \left(\frac{m-s}{kg}\right)^{0.312} {}^\circ\mathrm{K}^{0.344} \quad @t=60 \text{ s}$$

Since σ does not change appreciably with time, an average value of 129.5 was assumed.

The procedure to find T versus time is outlined below:

1. At time zero, both T and T_w are known. The thermal time constant, τ, can be found from equation (20).
2. A time interval ($\Delta t = 0.01$ s) was chosen and the new T was computed from equation (18).
3. The new wall temperature was calculated based on the procedure discussed earlier.[8]
4. Using the new values for T and T_w, a new value for τ was calculated from equation (20) and the procedure was repeated for other time steps.

Figure 9 shows the result of the above calculations for run number 22 (short dashed line). The temperature decay curve predicted by the variable time-constant computations is compared with the experimental data and the agreement is within 1.2°C (2.1°F). The experimental data points were obtained by measuring the gas pressure at discrete times and using the equation of state for nitrogen. Also shown in Fig. 9 is the resulting temperature decay curve if the overall time constant (15.6 s) is used for the entire process. This curve (long dashed line) overestimated the temperature from $t = 0$ to 15.6 s, and there is a crossover at $t = \tau_{\text{overall}}$ as expected.

The thermal time constant versus time for run number 22 is shown in Fig. 10. During the cooling process τ increases from 10.2 s at $t = 0$ to 41.9 s at $t = 60$ s. The rise in τ is due to a decrease in the Rayleigh number with a subsequent drop in the heat transfer coefficient.

It can be concluded from Fig. 9 that the thermal time-constant model is a powerful tool in predicting the gas temperature (or pressure) history. The use of a variable time constant will increase the accuracy appreciably without adding a great deal of complexity to the analysis.

Summary

A thermal time-constant model useful in accumulator calculations was discussed. The model requires a value for the time-constant, τ. This constant can be found experimentally for the accumulator at hand and for the specified range of operation. The time-constant correlation presented in this paper enables one to estimate τ and eliminates the need for experimental evaluation of this constant.

References

Beachley, N. H., 1973, "Graphical Determination of Accumulator Characteristics Using Real Gas Data," First Fluid Power Controls and Systems Conference, University of Wisconsin-Madison.

Copper, H. W., and Goldfrank, J. C., 1967, "B-W-R Constants and New Correlations," *Hydrocarbon Processing*, Vol. 46, No. 12, pp. 141–146.

Jacobsen, R. T. et al., 1973, *Thermophysical Properties of Nitrogen from the Fusion Line to 3500 R (1944 K) for Pressures to 150,000 psia (10342 × 10^5 N/m^2)*, National Bureau of Standards, Technical Note 648.

Kerr, C. P., 1986, "Procedure Estimates Benedict-Webb-Rubin Constants," *Oil and Gas Journal*, Vol. 84, No. 13, pp. 80–82.

Otis, D. R., 1973, "Predicting Performance of Gas Charged Accumulators," First Fluid Power Controls and Systems Conference, University of Wisconsin-Madison.

Otis, D. R., and Pourmovahed, A., 1985, "An Algorithm for Computing Nonflow Gas Processes in Gas Springs and Hydropneumatic Accumulators," ASME Journal of Dynamic Systems, Measurement and Control, Vol. 107, No. 1, pp. 93–96.

Pourmovahed, A., and Otis, D. R., 1984, "Effects of Thermal Damping on the Dynamic Response of a Hydraulic Motor-Accumulator System," ASME Journal of Dynamic Systems, Measurement and Control, Vol. 106, No. 1, pp. 21–26.

Pourmovahed, A., 1985, "Modeling the Transient Natural Convection in Gas-Filled, Variable Volume Cylindrical Enclosures with Applications to Hydraulic Accumulators," PhD thesis, Dept. of Mech. Engr., Univ. of Wisconsin-Madison.

Svoboda, J., Bouchard, G., and Katz, S., 1978, "A Thermal Model for Gas-Charged Accumulators Based on the Heat Conduction Distribution," *Fluid Transients and Acoustics in the Power Industry*, ASME Winter Annual Meeting, San Francisco, CA.

[7]The wall temperature varies with both time and position. The rise in the spatially averaged wall temperature is generally between 5 to 10 percent of the drop in the gas temperature. Thus, an estimate of the wall temperature is sufficient for this analysis. The spatially averaged wall temperature was estimated by setting the heat loss by the gas equal to the heat gain by the wall for any time step.

[8]The wall temperature did not change appreciably and could have been assumed constant for this test run.

Downloaded 28 Oct 2008 to 142.58.187.30. Redistribution subject to ASME license or copyright; see http://www.asme.org/terms/Terms_Use.cfm